Inorganica Chimica Acta 510 (2020) 119736

Contents lists available at ScienceDirect

Inorganica Chimica Acta

journal homepage: www.elsevier.com/locate/ica

Research paper

Synthesis, characterization, crystal structures and anti-diabetic activity of organotin (IV) complexes with 2-(4-hydroxynaphthylazo)-benzoic acid

Paresh Debnath[a], Keisham Surjit Singh[a,*], Thokchom Sonia Devi[b], S.Sureshkumar Singh[b], Ray J. Butcher[c], Lesław Sieroń[d], Waldemar Maniukiewicz[d,*]

[a] Department of Chemistry, National Institute of Technology Agartala, Jirania, Tripura (west) 799046, India
[b] Department of Forestry, North Eastern Regional Institute of Science And Technology, Nirjuli, Arunachal Pradesh 791109, India
[c] Department of Chemistry, Howard University, 525 College Street, NW, Washington DC 20059, USA
[d] Institute of General and Ecological Chemistry, Lodz University of Technology, 90-924 Lodz, Zeromskiego 116, Poland

ARTICLE INFO

Keywords:
Organotin(IV) complexes
Spectroscopy
Crystal structures
Antidiabetic activities

ABSTRACT

Three new organotin(IV) complexes **1–3** were synthesized by the reaction of 2-(4-hydroxynaphthylazo)-benzoic acid with *bis*-tributyltin(IV) oxide (**1**), dibutyltin(IV) oxide (**3**) or trimethyltin(IV) chloride (**2**), respectively. The complete characterization of the complexes was accomplished by elemental analysis, IR and multinuclear [^{1}H- and ^{13}C- and ^{119}Sn-] NMR spectroscopy. The crystal structures of all the complexes were elucidated with the help of X-ray single crystal diffraction analysis. The geometry around tin atoms in **1** and **2** was trigonal bipyramidal geometry where the equatorial plane was occupied by the three alkyl groups (Bu or Me) and the axial positions in **1** were being occupied by carboxylate and phenoxide oxygen atoms giving rise to a polymeric structure. In **2**, a hydroxy oxygen atom bridges two tin atoms occupying axial position while the other axial positions in each tin atom were being occupied by a carboxylate oxygen atom or oxygen atom of a water molecule respectively thereby completing trigonal bipyramidal geometry. The structure of **3** was a di-nuclear complex with six-co-ordinate distorted skew trapezoidal and seven-coordinate pentagonal bipyramidal geometry around the tin atoms, respectively. In the dinuclear structure, one of the tin atoms is coordinated by a terminal azo-ligand while the other tin atom is coordinated by two terminal azo-ligands. In addition to this, another azo-carboxylate ligand bridges the two atoms in the dinuclear structure. The NMR study showed that in the solution the complexes **1** and **2** adopted four-coordinate geometry, while in **3** there is five-coordinate structure. Complexes **1** and **3** were screened for their antidiabetic activities against α-glucosidase enzyme and results of the assay found that compound **3** exhibited significant inhibition activity.

1. Introduction

Organotin compounds particularly organotin(IV) carboxylates were found to exhibit important biological activities such as biocides, cytotoxicity, antimicrobial, anti-proliferation, antitumor, anticancer, anti-tuberculosis and anti-inflammatory [1–8]. Organotin(IV) carboxylates also displayed a wide range of intriguing structural diversity for instance they showed monomers, dimers, tetramers, hexameric, cyclic drum, ladder, 1D-, 2D- macro-cyclic structures etc. [8–13]. Moreover, diorganotin(IV) carboxylates [R = Me, *n*-Bu and Ph] with pyridine dicarboxylic acid exhibited interesting macro-cyclic hybrids having porous solid- state structures [14]. In addition to this, considerable attention have also been given to organotin(IV) compounds with azo-carboxylates because of their various intriguing molecular structures that exhibited as polymeric, monomeric, dimeric and macrocylic structures [15–20]. Organotin(IV) azo-carboxylates are also important for their potential biological applications as anti-cancer, cytotoxicity and toxicity on mosquito larvae [16–19]. Furthermore, in recent years our research group has been working on organotin compounds with some functionalized azo-carboxylates derived from 2- and 4- amino benzoic acids and their molecular structures and biological properties were studied [21–23]. The compounds were found to exhibit encouraging antimicrobial and antidiabetic activity and in some cases, they showed activity even better than standard drug compounds. In addition, more recently we have also studied chemistry of organotin compounds with some azo-carboxylates derived from 2- or 4-amino benzoic acids and naphthalen-2-ol [24–25]. The molecular structures of these organotin compounds were determined by X-ray crystallography.

* Corresponding authors.
E-mail addresses: surjitkeisham@yahoo.co.in (K.S. Singh), waldemar.maniukiewicz@p.lodz.pl (W. Maniukiewicz).

https://doi.org/10.1016/j.ica.2020.119736
Received 15 April 2020; Received in revised form 3 May 2020; Accepted 3 May 2020
Available online 06 May 2020
0020-1693/

The geometry around tin atoms in triorganotin complexes showed five coordinate distorted trigonal bipyramidal geometry [24] while crystal structure analysis of dibutyltin(IV) compounds with these ligand systems revealed structures ranges from five coordinate distorted trigonal bipyramidal geometry or six coordinate distorted octahedral or skew trapezoidal structures [25]. Therefore, as part of our ongoing research work on organotin chemistry with these functionalized azo-carboxylate ligands, now we are interested to explore further into the chemistry of organotin(IV) complexes with azo-carboxylate derived from 2-amino benzoic acid and naphthalen-1-ol. Herein, we employed naphthalen-1-ol (α-naphthol) as coupling moiety which introduces hydroxy group at 4-position in the naphthalene ring in the ligand framework. By employing this azo-carboxylate ligand for the synthesis of organotin (IV) compounds, we expect to get different structures from those organotin compounds [24] where hydroxy group is present at 2-position (naphthalen-2-ol) in the naphthalene ring of azo-carboxylate ligand framework which consequently would influence their biological activities. Thus bearing all these in mind, in this present report, we have synthesized three organotin(IV) compounds by reacting *bis*-tributyltin(IV) or dibutyltin(IV) oxide or trimethyltin(IV) chloride with this azo-carboxylate ligand functionalized at 4-position with hydroxy group in the naphthalene ring. The newly synthesized compounds were characterized with the help of elemental analysis, IR and multinuclear (^{1}H–^{13}C- and ^{119}Sn)-NMR spectroscopy. The structures of all organotin compounds were determined by X-ray crystallography and the results of study are discussed herein. Anti-diabetic activity of complexes **1** and **3** and the ligand was investigated using alpha- glucosidase enzyme and compared with standard drug and results of the assay are discussed in this contribution.

2. Experimental

2.1. Materials and methods

Dibutyltin(IV) oxide, *bis*-tributyltin(IV) oxide, tributyltin(IV) chloride, trimethyltin(IV) chloride, 2-amino benzoic acid, naphthalen-1-ol and triethyl amine were obtained from MERCK by purchase and were used without further purification. All solvents used for the reaction were dried following standard procedures. The elemental (Carbon, Hydrogen and Nitrogen) analyses were obtained from Perkin Elmer 2400 series II instrument. For recording IR spectra (4000–400 cm^{-1} using KBr discs) Shimadzu FT-IR-8400S spectrophotometer was employed. The multinuclear (^{1}H, ^{13}C and ^{119}Sn) NMR spectra were recorded on Bruker AMX 400 spectrometer measured at 400.13 for ^{1}H, 100.62 for ^{13}C and 149.18 MHz for ^{119}Sn-NMR using Me_4Si as reference for ^{1}H- and ^{13}C- chemical shifts set at 0.00 ppm while Me_4Sn set at 0.00 ppm was employed as reference for ^{119}Sn- chemical shifts.

2.2. Synthesis

2.2.1. Synthesis of 2-(4-hydroxynaphthylazo) benzoic acid (H_2L)

The azo-carboxylate ligand 2-(4-hydroxynaphthylazo) benzoic acid (H_2L) was prepared by usual diazo-coupling reaction of 2-amino benzoic acid with 1-naphthol following our analogous procedure [24,25]. To 5 g (36.45 mmol) 2-aminobenzoic acid, 12 mL concentrated HCl and 40 mL water was added and then digested on a water bath for about 1 h till the solution became clear. It was then kept in refrigerator for overnight and then diazotized at 0–5 °C with ice cold aqueous solution of $NaNO_2$ (2.51 g, in 20 mL water) for about 1 h. The diazotized solution was then added to 10% NaOH (5 g in 50 mL water) solution of 1-naphthol (5.256 g, 36.45 mmol) at about 0–2 °C with vigorous stirring to form a deep red colored solution and it was continued under stirring condition for about 3 h. The reaction mixture was again kept in refrigerator for overnight. After 2–3 h at room temperature, the reaction mixture was acidified with dilute acetic acid to form the red precipitate of the desired azo-ligand. The final product was then filtered, washed with distilled water for several hours till it became neutral and finally the product was dried on water bath. The azo ligand was then recrystallized from methanol to get the pure deep red crystalline product of the ligand. Yield: 7.9 g, 74%; m.p.: 232–234 °C. Anal. calcd. for $C_{17}H_{12}N_2O_3$: C, 69.86; H, 4.14; N, 9.58%. Found: C, 69.54; H, 4.21; N, 9.43%.IR (KBr, cm^{-1}): 3416 ν(OH), 1673 $\nu(COO)_{asy}$, 1455 ν(N=N), 1187 ν(C−O). ^{1}H NMR (DMSO-d_6, 400.13 MHz) δ_H: 12.9 [s, 1H, OH], 8.49 [d, 1H, H-9, J = 7.6 Hz], 8.06 [d, 1H, H-6, J = 7.6 Hz], 7.92 [m, 2H, H-2, H-3́], 7.72 [m, 2H, H-7, H-8], 7.64 [t, 1H, H-4′, J = 7.6 Hz], 7.55 [t, 1H, H-5́, J = 7.6 Hz], 7.18 [m, 1H, H-6́], 6.79 [d, 1H, H-3, J = 8.8 Hz] ppm; Signal for –COOH proton could not be detected due to rapid solvent exchange. ^{13}C NMR (DMSO-d_6, 100.62 MHz) δ_C: 179.9 [COO], 169.8 [C-4],146.1 [C-1′], 134.5 [C-1], 134.1 [C-5́], 133.8 [C-10], 131.3 [C-3′], 130.8 [C-4′], 128.4 [C-6], 115.0 [C-3]; other signals: 127.5, 124.6, 122.0, ppm. The structural formula and numbering scheme for the H_2L is shown in Scheme 1.

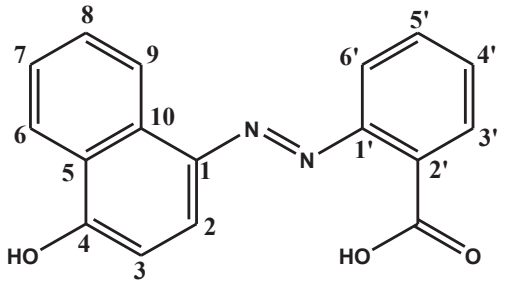

2-(4-hydroxynaphthylazo) benzoic acid (H_2L)

Scheme 1. The structural formula and numbering scheme for the ligand H_2L.

2.2.2. Synthesis of Bu_3SnHL (1)

Tributyltin(IV) compound **1** was synthesized by the reaction of *bis*-tributyltin(IV) oxide with 2-(4-hydroxynaphthylazo) benzoic acid [H_2L] in (M: L = 1:1) molar ratio in refluxing condition by using Dean-Stark moisture trap apparatus. In this process, 2-(4-hydroxynaphthylazo) benzoic acid (0.147 g, 0.503 mmol) was added to 50 mL anhydrous toluene in a round bottom flask on an oil bath fitted with the Dean-Stark apparatus and was refluxed for 30 min to get a red colored suspension. Then, *bis*-tributyltin (IV) oxide (0.3 g, 0.503 mmol) was added to the suspended solution with continuous stirring. Stirring was continued for 6 h and the water produced during reaction was trapped by the Dean-Stark receiver. The red colored solution was then filtered and filtrate was kept for about 7 days to get dark red crystals of the desired complex **1.** Yield: 0.47 g, 88%; m.p.: 110–112 °C. Anal. calcd. for $C_{29}H_{38}N_2O_3Sn$: C, 49.92; H, 6.59; N, 4.82%. Found: C, 49.30; H, 6.35; N, 4.55%. IR (KBr, cm^{-1}): 3440 ν(N−H str.), 2921 ν(C−H str. of Bu), 1622 $\nu(COO)_{asym}$, 1447 ν(N=N), 1351 $\nu(COO)_{sym}$ 1149 ν(C−O), 676 ν(Sn-C), 495 ν(Sn-O).^{1}H NMR ($CDCl_3$, 400.13 MHz) δ_H, Ligand skeleton: 13.08 [s, 1H, OH], 8.48 [d, 1H, H-9, J = 8.4 Hz], 8.20 [d, 1H, H-6, J = 8.0 Hz], 8.06 [d, 1H, H-3′, J = 6.8 Hz], 7.99 [d, 1H, H-8, J = 8.4 Hz], 7.73[d, 1H, H-2, J = 10.4 Hz], 7.65 [t, 1H, H-7, J = 7.6 Hz], 7.55 [t, 1H, H-4′, J = 7.6 Hz], 7.49[t, 1H, H-5′, J = 7.6 Hz], 7.01[t, 1H, H-6′, J = 7.6 Hz], 6.74[d, 1H, H-3, J = 10.4 Hz]; Sn-^{n}Bu Skeleton: 1.71[m,6H, H-α], 1.40 [m, 12H, H-β & H-γ], 0.94 [t, 9H, H-δ] ppm. ^{13}C NMR ($CDCl_3$, 100.62 MHz) δ_C: 185.1 [COO], 173.1 [C-4],145.5 [C-1′], 135.9 [C-1], 134.1 [C-5́], 133.4 [C-10], 132.5 [C-3′], 132.1 [C-4′], 130.2 [C-6], 129.6 [C-8], 127.8 [C-7], 126.0 [C-2′], 124.5 [C-2], 122.9 [C-5], 121.0 [C-9], 114.6 [C-6′], 114.0 [C-3]; Sn-^{n}Bu Skeleton: 27.9 [C-β], 27.0 [C- γ] ^{3}J [^{119}Sn-^{13}C(63.3 Hz)], 17.0 [C-α] ^{1}J [^{119}Sn-^{13}C(344.1 Hz)], 13.7 [C-δ] ppm. ^{119}Sn NMR ($CDCl_3$, 149.18 MHz): + 127.19 ppm.

2.2.3. Synthesis of $[(CH_3)_3Sn]_2(OH)(H_2O)HL$ (2)

The compound **2** was synthesized by the reaction of trimethyltin(IV)

chloride with 2-(4-hydroxynaphthylazo) benzoic acid using triethylamine as base under refluxing condition with (M:L = 2:1) molar ratio. In this procedure, 2-(4-hydroxynaphthylazo) benzoic acid (0.219 g, 0.752 mmol) was dissolved in 30 mL anhydrous methanol in a round bottom flask in presence of triethylamine base (0.152 g, 1.505 mmol) and was refluxed on an oil bath for about 30 min with an equipped water cooled condenser. Then, trimethyltin(IV) chloride (0.3 g, 1.5055 mmol) was then added to the reaction mixture with continuous stirring. It was again refluxed for about 6 h and then filtered. The precipitate containing $Et_3N.HCl$ was filtered off and the filtrate was then collected, evaporated to dryness. The final product was washed by hexane to get the pure deep red crystalline product. The small crystalline product obtained after purification was then recrystallized from anhydrous methanol to obtain pure red crystals of the complex **2.** Yield: 0.672 g, 68%; m.p.: 216–217 °C. Anal.calcd. for $C_{23}H_{32}N_2O_5Sn_2$: C, 42.24; H, 4.93; N, 4.28%. Found: C, 42.67; H, 4.32; N, 4.13%. IR (KBr, cm^{-1}): 3439 ν(NH), 2923 ν(C—H str. of Sn-CH_3), 1639 $\nu(COO)_{asy}$, 1450 ν(N═N), 1352 $\nu(COO)_{sym}$ 1160 ν(C—O), 681 ν(Sn-C), 522 ν(Sn-O). ^{1}H NMR ($CDCl_3$, 400.13 MHz) δ_H, Ligand skeleton: 8.43 [d, 1H, H-9, J = 8.0 Hz], 8.28 [d, 1H, H-6, J = 7.6 Hz], 8.12 [d, 1H, H-3, J = 8.0 Hz], 7.59 [m, 2H, H-7, H-8], 7.48[m, 2H, H-2 , H-4′], 7.37 [m, 1H, H-5′], 7.16 [t, 1H, H-6′, J = 8.0 Hz], 6.67[d, 1H, H-3, J = 10.0 Hz]; Sn-CH_3Skeleton: 0.75 [s, 9H, (Sn-CH_3)] ^2J [^{119}Sn-^{1}H (57.21 Hz)] ppm. ^{13}C NMR ($CDCl_3$, 100.62 MHz) $\delta_{C,}$ Ligand skeleton: 179.2 [COO], 173.7 [C-4],144.2 [C-1′], 141.8 [C-1], 134.3 [C-5′], 133.7 [C-10], 133.3 [C-3′], 132.5 [C-4′], 129.1 [C-6], 128.7 [C-8], 128.4 [C-7], 127.5 [C-2′], 126.5 [C-2], 125.6 [C-5], 124.1 [C-9], 122.4 [C-6′], 116.3 [C-3]; Sn-CH_3 Skeleton: −1.7 [Sn-CH3] ppm. ^{119}Sn NMR ($CDCl_3$, 149.18 MHz): + 139.21 ppm.

2.2.4. Synthesis of $[Bu_2Sn(HL)_2]_2$ (3)

Dibutyltin(IV) compound **3** was synthesized following analogous procedure as in case of compound **1** where dibutyltin(IV) oxide (0.3 g, 1.20 mmol) was used instead of *bis*-tributyltin(IV) oxide with 2-(4-hydroxynaphthylazo) benzoic acid (0.704 g, 2.41 mmol) in (M:L = 1:2) molar ratio fixed with the Dean-Stark apparatus under refluxing condition to get deep red compound **3**. Yield: 0.67 g, 84%; m.p.: 211–212 °C. Anal.calcd. for $C_{84}H_{80}N_8O_{12}Sn_2$: C, 61.86; H, 4.94; N, 6.87%. Found: C, 61.73; H, 5.1; N, 6.81%. IR (KBr, cm^{-1}): 3139 ν(N—H str.), 2921 ν(C—H str. of Bu), 1627 $\nu(COO)_{asym}$, 1475 ν(N═N), 1440 $\nu(COO)_{sym}$ 1178 ν(C—O), 675 ν(Sn-C), 501 ν(Sn-O).^{1}H NMR ($CDCl_3$, 400.13 MHz) δ_H, Ligand skeleton: 12.5 [s, 1H, OH], 8.48 [d, 1H, H-9, J = 8.0 Hz], 8.17 [m, 2H, H-2 & H-3′], 8.04 [d, 1H, H-6, J = 8.0 Hz], 7.67 [m, 3H, H-7, H-8 & H-4′], 7.51[t, 1H, H-5′, J = 7.6 Hz], 7.11 [t, 1H, H-6′, J = 7.6 Hz], 6.74 [d, 1H, H-3, J = 10 Hz]; Sn-^{n}Bu Skeleton: 1.95[m,2H, H-α], 1.82 [m, 2H, H-β], 1.50 [m, 2H, H-γ], 0.93 [t, 3H, H-δ] ppm. ^{13}C NMR ($CDCl_3$, 100.62 MHz) δ_C: 184.9 [COO], 176.7 [C-4],145.8 [C-1′], 135.6 [C-1], 134.1 [C-5́], 132.8 [C-10], 132.3 [C-3′], 130.2 [C-4′], 129.0 [C-6], 128.2 [C-8], 126.1 [C-7], 125.3 [C-2′], 123.9 [C-2], 123.0 [C-5], 121.3 [C-9], 114.5 [C-6′], 112.4 [C-3]; Sn-^{n}Bu Skeleton: 26.9 [C-β], 26.4 [C- γ], 21.4 [C-α], 13.6 [C-δ] ppm. ^{119}Sn NMR ($CDCl_3$, 149.18 MHz): −133.39 ppm. The numbering scheme of Sn-Bu skeletal in the tributyltin(IV) and dibutyltin(IV) complexes is shown below

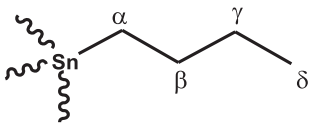

2.3. Crystallographic data collection and structure refinement

Single crystal X-ray diffraction data were collected by the ω-scan technique using MoK_α (λ = 0.71073 Å) radiation. The $\mathbf{H_2L}$ salt and **1** crystals were studied at 100 K using a RIGAKU XtaLAB Synergy, Dualflex, Pilatus 300 K diffractometer [26] with Photon Jet micro-focus X-ray Source while the crystals **2** and **3** were measured using a Bruker AXS Smart APEX-II CCD diffractometer [27]. Data collection, cell refinement, data reduction and absorption correction were carried out using CrysAlis PRO software [26] for $\mathbf{H_2L}$ and **1.** Whereas the SMART and SAINT-PLUS [28] programs were used for **2** and **3**, respectively. The crystal structures were solved by using direct methods with the SHELXT 2018/2 program [29]. Atomic scattering factors were taken from the International Tables for X-ray Crystallography. Positional parameters of non-H-atoms were refined by a full-matrix least-squares method on F^2 with anisotropic thermal parameters by using the SHELXL 2018/3 program [30]. All hydrogen atoms were placed in calculated positions (C—H = 0.93–0.98 Å) and included as riding contributions with isotropic displacement parameters set to 1.2–1.5 times the U_{eq} of the parent atom. Despite many attempts to crystallize, the quality of crystals used in the analysis was not very good, therefore there were some problems with refining the structures. In structure **1**, a disorder in one of the butyl groups was observed. Thus the ellipsoids of some C atoms in the disordered region were odd-shaped. The SIMU restraints have been applied in the refinement and a slight improvements in shape o ellipsoids was obtained. The disorder ratio was 0.731(9):0.269(9). In structure **2** all attempts to model the disorder in water molecule in order to find proper positions of hydrogen atoms failed. So, we decided to bypass these hydrogen atoms from the model of structure during the refinement. In addition, for 2 and ligand salt data twin refinement was required. In **1 and 3** contribution of highly disordered solvent (presumably toluene and/or water), which could not be modeled, was removed by SQUEEZE routine using PLATON [31]. For structure **1**, the three voids of about 350 $Å^3$ each containing 59 electrons were found. Whereas for structure **3** the one void volume was 520 $Å^3$ and contained 125 electrons. Crystal data and structure refinement parameters are shown in Table 1, while selected geometric parameters are collected in Table 2. Hydrogen bonding parameters are presented in Table 3.

2.4. Anti-diabetic assay

Anti-diabetic activities of compounds **1–3** and standard drug acarbose were screened following the 96-well microplate-based α-glucosidase assay as described by Kumar *et al.*[32] and also using our earlier antidiabetic assay [25]. In this method, 1 mg of each compound was dissolved in 20 μL DMSO (D) and Ethanol (E) and diluted to 1000 μL in a 2 mL Eppendorf tube with sterile water (Milli-Q) and these samples were employed for the enzyme assay. Studies of the α-glucosidase enzyme inhibition assay were performed in a reaction volume of 75 μL using 96-well microplate. In this method, 25 μL each of sample solution and α-glucosidase enzyme (0.5U) were gently mixed and pre-incubated at 37 °C ± 1 °C for 10 min. Then, 25 μL of the substrate (0.5 mM, *p*-nitrophenyl α-D glucopyranoside, PNPG) was added to the reaction mixture and incubated again at 37 °C ± 1 °C for 30 min. After this, by adding 100 μL of 0.2 M sodium carbonate solution, the reaction was terminated. The amount of *p*-nitrophenol released from PNPG (yellow colour) was then quantified on a 96-well microplate at 405 nm using UV visible spectrophotometer (Mustikan GO, Thermo-Scientific, Finland). The α-glucosidase inhibitor drug (Acarbose, ACB) was employed as standard reference. All reactions were performed in five replicates. The percentage of α-glucosidase inhibition activity was calculated with the help of the formula i.e. α-glucosidase inhibition activity (%) = [(Control OD-Sample OD) / Control OD] x100) where Control OD = OD of the control reaction without inhibitor-Blank OD; Sample OD = Sample OD-Sample blank OD]. Similarly, the experiment for dose–effect analysis of antidiabetic activity was performed using *in vitro* α-glucosidase assay in a reaction volume of 75 μL using 96-well microplate as described above. A sample solution of 5, 10, 15, 20 and 25 μL (~67, 133, 266 and 333 μg/mL) were mixed with 25 μL of the α-

Table 1
Crystal data and structure refinement parameters for the **H_2L** salt and complexes **1**, **2** and **3**.

Parameters	H_2L salt	1	2	3
Empirical formula	$C_{23}H_{31}N_3O_5$	$C_{29}H_{38}N_2O_3Sn$	$C_{24}H_{36}N_2O_6Sn_2$	$C_{84}H_{80}N_8O_{12}Sn_2$
Formula weight	429.51	581.32	685.97	1630.94
Temperature(K)	100(3)	100(3)	100(3)	296(2)
Crystal system	Triclinic	Trigonal	Triclinic	Triclinic
Space group	*P*-1	*R*3*c*	*P*-1	*P*-1
a (Å)	10.7854(3)	38.4630(3)	7.5426(4)	12.6862(4)
b (Å)	13.5964(3)	38.4630(3)	12.1092(7)	19.2092(7)
c (Å)	15.4929(3	10.2363(1)	15.8208(9)	19.2904(7)
α (°)	103.894(2)	90	97.935(2)	63.733(2)°
β (°)	90.498(2)	90	92.760(2)	78.236(2)°
γ(°)	91.519(2)	120	107.510(2)	88.210(2)°
Volume(Å^3)	2204.41(9)	13114.8(3)	1358.68(13)	4117.6(3)
Z	4	18	2	2
Density(Mg/m^3)	1.294	1.325	1.677	1.315
Absorp. coeff.(mm^{-1})	0.092	0.906	1.877	0.669
F(0 0 0)	920	5400	684	1672
Crystal size (mm^3)	0.55 × 0.28 × 0.21	0.22 × 0.28 × 0.33	0.08 × 0.25 × 0.29	0.10 × 0.10 × 0.05
Radiation	MoK_α(λ = 0.71073)	MoK_α(λ = 0.71073)	MoK_α(λ = 0.71073)	MoK_α(λ = 0.71073)
Theta range for data collection	2.31 to 25.03°	2.56 to 25.02°	1.30 to 25.02°	2.13 to 24.74°
Index ranges	$-12 \le h \le 12$, $-16 \le k \le 16$, $-18 \le l \le 18$	$-45 \le h \le 45$, $-45 \le k \le 45$, $-12 \le l \le 12$	$-8 \le h \le 8$, $-14 \le k \le 14$, $0 \le l \le 18$	$-14 \le h \le 14$, $-22 \le k \le 22$, $-22 \le l \le 22$
Reflection collected	31,156	131,510	9917	93,972
Independent reflections	15,389 [R(int) = 0.0858]	5150 [R(int) = 0.031]	4588 [R(int) = 0.0127]	13,973 [R(int) = 0.0858]
Goodness of fit on F^2	1.061	1.10	1.15	0.98
Final R indices[I greater than 2sigma(I)]	R1 = 0.0585, w*R*2 = 0.1771	R1 = 0.0130, w*R*2 = 0.0342	R1 = 0.0236, w*R*2 = 0.0785	R1 = 0.0577, w*R*2 = 0.1352
R indices(all data)	R1 = 0.0665, w*R*2 = 0.1854	R1 = 0.0131, w*R*2 = 0.0343	R1 = 0.0242, w*R*2 = 0.0798	R1 = 0.1284, w*R*2 = 0.1598
Largest diff. peak and hole(eÅ^{-3})	0.315 and −0.312	0.375 and −0.258	0.636 and −0.584	0.688 and −0.458

glucosidase enzyme (0.5U) and then volume was made up to 75 μL with assay buffer. The reaction mixture was pre-incubated at 37 °C ± 1 °C for 10 min and then 25 μL of the substrate (0.5 mM, PNPG) was added to the reaction mixture and incubated at 37 °C ± 1 °C for 30 min. The reaction was terminated adding 100 μL of 0.2 M sodium carbonate solution. Amount of *p*-nitrophenol released from PNPG was quantified on a 96-well microplate at 405 nm on a UV visible spectrophotometer (Mustikan GO, Thermo-Scientific, Finland). All reactions were performed in five replications. The percentage of α-glucosidase inhibition activity was calculated by using the same formula as mentioned above.

Table 2
Selected bond lengths (Å) and bond angles (°) for **H_2L** salt and the tri or diorganotin (IV) complex **1**, **2** and **3**.

Atoms	H_2LBond Length (Å)	Atoms	1Bond Length (Å)	Atoms	2Bond Length (Å)	Atoms	3Bond Length (Å)
N1-N2	1.334(3)	Sn1-O1	2.148(2)	Sn1-O1	2.275(5)	Sn1-O1	2.479(5)
O1-C1	1.273(3)	Sn1-O3$^{\#1}$	2.537(3)	Sn1-O4	2.188(5)	Sn1-O2	2.165(4)
O2-C1	1.255(3)	Sn1-C18	2.143(3)	Sn2-O4	2.136(5)	Sn1-O4	2.506(4)
O3-C11	1.230(3)	Sn1-C22	2.151(3)	Sn2-O5	2.402(5)	Sn1-O5	2.188(4)
N1-C7	1.389(3)	Sn1-C26	2.134(3)	Sn1-C18	2.138(8)	Sn1-O9	2.690(5)
N2-C8	1.306(4)			Sn1-C19	2.134(8)	Sn2-O7	2.089(4)
N3-N4	1.330(3)			Sn1-C20	2.139(8)	Sn2-O8	2.627(5)
O4-C21	1.268(3)			Sn2-C21	2.132(7)	Sn2-O10	2.104(4)
O5-C21	1.257(3)			Sn2-C22	2.120(8)	Sn2-O11	2.467(5)
O6-C31	1.231(3)			Sn2-C23	2.123(8)	Sn1-C35	2.074(8)
N3-C27	1.389(3)					Sn1-C39	2.096(7)
N4-C28	1.307(3)					Sn2-C77	2.096(9)
						Sn2 -C81	2.095(8)
Atoms	H_2L Bond Angle (°)	Atoms	1 Bond Angle (°)	Atoms	2 Bond Angle (°)	Atoms	3 Bond Angle (°)
N2-N1-C7	119.6(2)	O1-Sn1-O3$^{\#1}$	171.20(8)	O1-Sn1-O4	176.31(19)	O1-Sn1-O2	55.36(13)
N1-N2-C8	120.0(2)	C22-Sn1-C26	123.84(11)	O1-Sn1-C18	89.1(2)	O1-Sn1-O9	85.77(15)
N1-C7-C6	121.0(2)	O1-Sn1-C18	92.02(10)	O1-Sn1-C19	90.4(3)	O2-Sn1-O5	79.07(14)
N2-C8-C9	126.1(2)	O1-Sn1-C22	100.91(10)	O1 -Sn1-C20	85.1(2)	O4-Sn1-O5	55.57(13)
N2-C8-C17	116.2(2)	C18-Sn1-C22	116.49(11)	C18-Sn1-C19	123.7(3)	O4-Sn1-O9	84.15(15)
N4-N3-C27	119.5(2)	C18-Sn1-C26	115.56(12)	O4-Sn2-O5	179.5(2)	O7-Sn2-O8	54.34(19)
N3-N4-C28	120.5(2)	O3$^{\#1}$-Sn1-C18	81.90(10)	O4-Sn2-C21	93.3(2)	O7-Sn2-O10	80.24(18)
N3-C27-C26	120.3(2)	O3$^{\#1}$-Sn1-C26	80.18(10)	O4-Sn2-C22	95.0(3)	C35-Sn1-C39	156.5(3)
N4-C28-C29	126.0(2)	O3$^{\#1}$-Sn1-C22	87.54(9)	O4-Sn2-C23	95.9(3)	C77-Sn2-C81	135.5(3)
N4-C28-C37	116.0(2)			C22-Sn2-C23	120.8(3)		

(#1) 1/3-x + y,5/3-x,2/3 + z;

Table 3
Hydrogen bonding parameters for the **H_2L** salt and tri- or diorganotin(IV) complex **1**, **2** and **3**.

Compound	D-H…..A	d(D-H)	d(H….A)	d(D…A)	< (DHA)
H_2L salt	N(1)-H(1 N)…O(2)	0.88	1.97	2.650(3)	133
	N(3)-H(3 N)…O(5)	0.88	.98	2.648(3)	132
	N(5)-H(5 N)…O(1)	1.00	1.66	2.655(3)	174
	N(6)-H(6 N)…O(4)	1.00	1.70	2.693(3)	171
	O(7)-H(7A)…O(8)^{I}	0.85	1.96	2.803(3)	169
	O(7)-H(7B)…O(1)	0.85	1.96	2.807(3)	173
	O(8)-H(8A)…O(7)	0.85	1.96	2.791(3)	166
	O(8)-H(8B)…O(5)	0.85	1.96	2.837(3)	177
	O(9)-H(9A)…O(4)	0.85	1.95	2.792(3)	170
	O(9)-H(9B)…O(10)	0.85	1.95	2.779(4)	164
	O(10)-H(10B)…O(2)^{II}	0.85	2.00	2.845(3)	170
	C(4)-H(4)…O(5)^{I}	0.95	2.56	3.498(3)	169
	C(24)-H(24)…O(2)^{II}	0.95	2.55	3.481(3)	165
1	N(1)-H(1)…O(2)	0.86(3)	1.84(4)	2.600(3)	145(3)
	C(23)-H(23A)…O(3)^{III}	0.99	2.56	3.285(4)	130
2	N(1)-H(1)…O(2)	0.88	1.90	2.592(7)	134
	O(1 M)-H(1 M)…O(2)	0.84	1.92	2.734(8)	163
	O(5 W)…O(3)^{IV}	———	———	2.842(7)	——
	O(5 W)…O(3)^{V}	———	———	3.001(7)	——
	O(4)-H(4O)…O(1 M)^{VI}	0.84	1.98	2.789(8)	163
	C(12)-H(12A)…O (5)^{VII}	0.95	1.95	2.897(8)	170
3	N(2)-H(2A)…O(2)	0.86	1.95	2.612(6)	133
	N(3)-H(3A)…O(4)	0.86	1.95	2.613(6)	133
	N(5)-(H5A)…O(8)	0.86	1.98	2.638(7)	133
	N(8)-H(8A)…O(10)	0.86	1.98	2.638(7)	132

$^{(I)}$1-x,1-y,2-z; $^{(II)}$ 1-x,1-y,1-z $^{(III)}$ 1/3-x + y,5/3-x,2/3 + z; $^{(IV)}$2-x,1-y,1-z; $^{(V)}$ x,1 + y,1 + z; $^{(VI)}$ 1-x,1-y,1-z; $^{(VII)}$ x,-1 + y,-1 + z;

3. Results and discussion

3.1. Synthesis

Tributyltin(IV) complex (**1**) and dibutyltin(IV) complex (**3**) were synthesized by reacting 2-(4-hydroxynaphthylazo) benzoic acid with *bis*-tributyltin(IV) oxide and dibutyltin(IV) oxide in anhydrous toluene using dean and stark apparatus in molar reaction ratio (1:1) and (1:2) M:L respectively. On contrary, trimethyltin(IV) complex (**2**) was synthesized by reacting the ligand with trimethyltin(IV) chloride in anhydrous methanol using triethylamine base in 2:1 (M: L) molar reaction ratio. Complex **1** was also prepared adopting different reaction route by reacting tributyltin(IV) chloride with the ligand in presence of Et_3N base with lesser yield compared to the previous method. So, we adopted first method for the synthesis of **1**. All the complexes were obtained in good yield and found to have good solubility in most of the common organic solvents. The reaction scheme for the synthesis of complexes **1–3** is shown in Scheme 2.

3.2. Spectroscopic characterization

3.2.1. IR spectroscopy

The IR spectroscopic data for azo-carboxylate ligand and compounds **1–3** are provided in the experimental section. IR spectroscopy is an important useful tool for determining the coordination behavior of carboxylate ligand as monodentate or bidentate in complexes in solid state [15,23,24,33,34]. The asymmetric [ν_{asy}(COO)] stretching absorption band of the ligand was observed at 1673 cm^{-1} and in the complexes **1–3**, this band was shifted to lower frequency range at 1622–1639 cm^{-1} which indicates the carboxylate coordination to Sn-atom in the complexes [16,17,23]. Usually, carboxylate displays two type of bands, one strong asymmetric stretching band [ν_{asy}(COO)] at 1580–1650 cm^{-1} and a weaker symmetric stretching band [ν_{sym}(COO)] near 1320–1450 cm^{-1} [15,23,24,33,34]. Moreover, $\Delta\nu$[ν_{asy}(COO)- ν_{sym} (COO)] value can be used for determining the coordination behavior of carboxylate ligand. If this value is below 200 cm^{-1}, then it indicates a bi-dentate mode of coordination while if $\Delta\nu$ is greater than 200 cm^{-1}, then the presence of mono-dentate mode of coordination of the carboxylate ligand to the tin atom can be assigned in the complexes [21,24,33,34]. The typical ν_{asy}(COO) asymmetric stretching frequency bands for complexes **1** and **2** were observed at 1622 and 1639 cm^{-1} while the symmetric stretching absorption bands observed at 1351 cm^{-1} and 1352 cm^{-1} and their corresponding $\Delta\nu$ was found to be 271 cm^{-1} and 287 cm^{-1} respectively. Hence it can be suggested, that in complexes **1** and **2**, the carboxylate ligand coordinate to Sn-atom in mono-dentate mode of coordination [21,35]. Furthermore, complex **3** shows asymmetric IR stretching frequency band at 1627 cm^{-1} while the symmetric stretching frequency band at 1440 cm^{-1} and the value of $\Delta\nu$ was found to be 187 cm^{-1}. This suggests bi-dentate mode of coordination of carboxylate ligand to the Sn-atom in complex **3** [21–24,35]. The coordination mode of carboxylate ligands in these complexes were found to be in fully consistent with the single crystal structures of the complexes (*vide infra*). Moreover, the IR absorption bands observed in the range 675–681 cm^{-1} and 495–522 cm^{-1} in complexes **1–3** are assigned for Sn-C and Sn-O respectively [23,36,37].

3.2.2. Multinuclear (^1H, ^{13}C and ^{119}Sn) NMR spectroscopy

^1H-, ^{13}C- NMR spectroscopic characterization data of the azo-carboxylate ligand was recorded in DMSO-d_6 while ^1H, ^{13}C and ^{119}Sn NMR spectroscopic data for the complexes **1–3** were recorded in $CDCl_3$ and their spectroscopic data are provided in the experimental section. Some representative spectra for the ligand and complexes were also provided in the Electronic Supplementary Information (ESI). The assignments of ^1H-, ^{13}C- NMR spectra of the ligand was accomplished by examining its chemical shift values, integration values, multiplicity patterns and also by careful comparison of the proton NMR spectroscopic data of similar type of azo-ligands derived from either 2-amino benzoic acid [21,23,24] or 1-naphthol reported earlier [38–40]. The assignments of the chemical shift position of the protons and carbons for the complexes were achieved by examining their chemical shift values, integration values, multiplicity patterns and also by comparing ligand NMR data with those of the complexes because of the similarity in their spectral data. The ^1H NMR spectroscopic data for aromatic protons in complexes were obtained in the range 6.67–8.48 ppm. In case of complexes **1** and **3**, the tin butyl protons showed a triplet and multiplet peaks in the range 0.93–0.94 ppm and 1.40–1.95 ppm which can be attributed to methyl and three methylene protons of the tin butyl protons respectively [23,24]. In complex **2**, a singlet peak was observed at 0.75 ppm which is assigned to tin-methyl protons [21,24]. The ^{13}C NMR spectra of the azo carboxylate ligand showed δ (COO) signal at 179.9 ppm but in case of complexes **1–3**, the δ (COO) signals were appeared in the range 179.2–179.9 ppm. The ^{13}C NMR signals for aromatic ring carbons of the free azo carboxylate ligand was observed in the range 115.0–169.8 ppm whereas in case of complexes **1–3**, these signals were observed in the range 114.0–176.7 ppm. The number of ^1H and ^{13}C NMR signals observed in the ligand and the complexes were found to be in consistent with the formulation of expected compounds. The geometry and coordination number around tin atoms in solution state for tin complexes can be determined by using $^2J(^{119/117}Sn\text{-}^1H)$ and ^nJ ($^{119}Sn\text{-}^{13}C$) coupling constants [16,21,41–44]. It is commonly observed that four coordinate tributyltin compounds exhibit $^1J(^{119/117}Sn\text{-}^{13}C)$

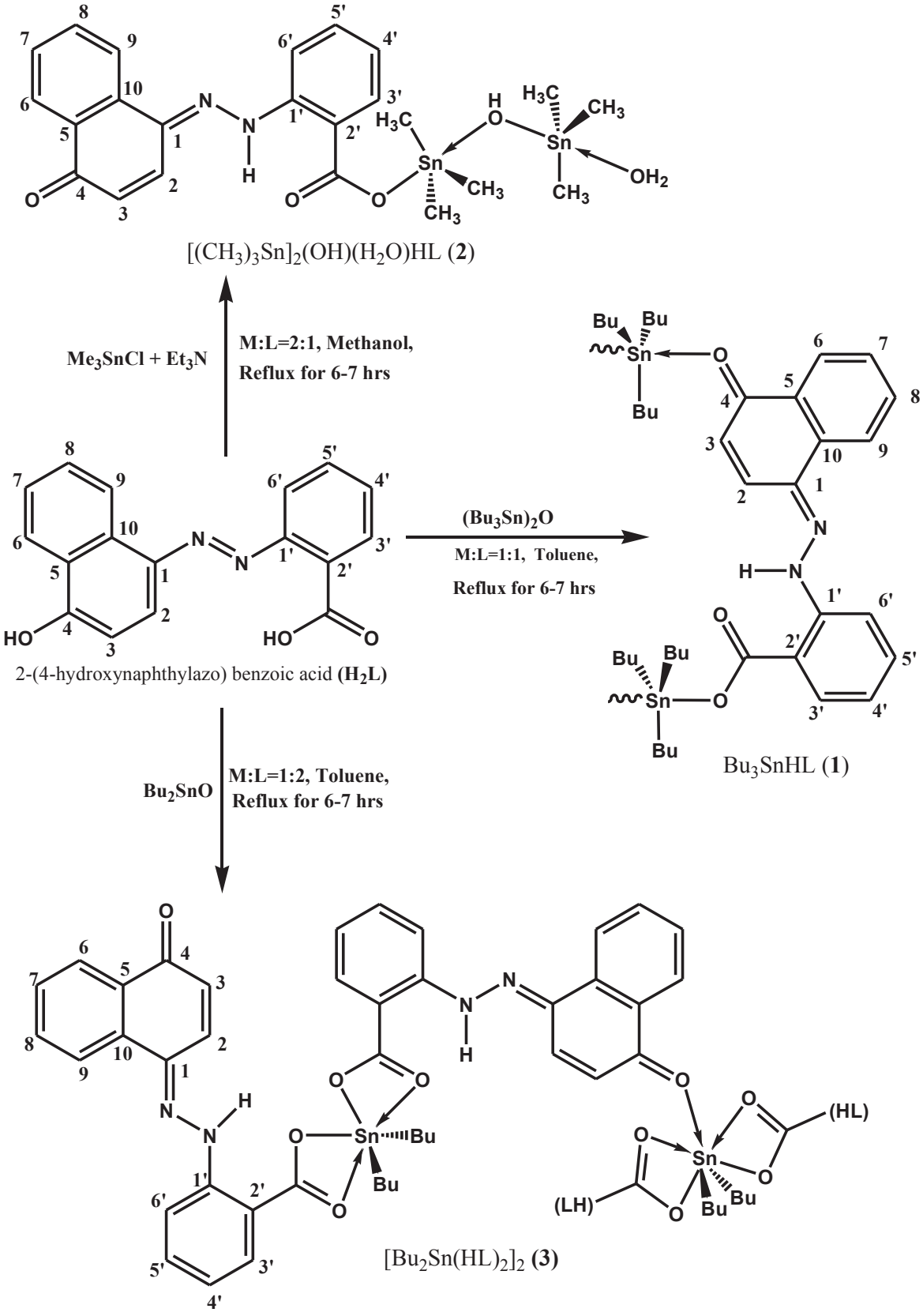

Scheme 2. Reaction scheme for the synthesis of compounds **1**, **2** and **3**.

coupling in the range of 325–390 Hz and five coordinated ones in the range of 430–540 Hz while four coordinate trimethyltin compounds display ^{2}J ($^{119/117}$Sn-^{1}H) coupling in the range 40–59 Hz [16,21,42–46]. In case of complex **1**, the ^{1}J (^{119}Sn-^{13}C) and ^{3}J (^{119}Sn-^{13}C) coupling satellites were observed at 344.1 Hz and 63.3 Hz respectively which is in consistent with the four coordinate tetrahedral

geometry of the tin atom in solution state for the given complex [21–24,42–44]. In addition, complex **2** displays $^{2}J(^{119}Sn\text{-}^{1}H)$ coupling (57.2 Hz) suggesting the 4-coordinate tetrahedral geometry of Sn-atom in solution state [22,45–46]. However, $^{2}J(^{119}Sn\text{-}^{1}H)$ values for complexes **1** and **3**, $^{n}J(^{119}Sn\text{-}^{13}C)$ couplings for the complexes **2** and **3** could not be assigned because of the poor signal-to-noise ratio and also low intensities of the Sn-Bu resonances [18,23]. Furthermore, the geometry around tin atom in organotin compounds in solution state can also be determined by calculating angle between C-Sn-C using Lockhart and Mander's equation [47] $\{\theta(\text{C-Sn-C}) = 0.0161 \mid {}^{2}J(\text{Sn-H}) \mid^{2} - 1.32 \mid {}^{2}J(\text{Sn-H}) \mid + 133.4\}$. In case of complex **2**, the calculated angle was found to be 110.57° indicating the four coordinated tetrahedral geometry [21,22,42,47]. The geometry of the complexes was also further confirmed by ^{119}Sn NMR study from δ (^{119}Sn) values of the complexes. Generally, if δ(^{119}Sn) values are found in the range −210 to −400 ppm, the geometry corresponds for six coordinate, −90 to −190 for five coordinate and − 60 to + 200 ppm were assigned for four coordinate geometry of tin in organotin complexes [18,23,24,48]. The ^{119}Sn chemical shift values for the complexes **1**, **2**, and **3** were observed at + 127.2, +139.2 and −133.4 ppm respectively. Hence, the geometry around tin atom for complexes **1** and **2** are suggested to adopt four coordinate structure in solution state [21,24,43–45] while in case of **3**, the geometry is five coordinate and the observed tin chemical shift values are also in consistent with those for other reported $R_2Sn[O_2CR']_2$ type complexes [18,49–52].

3.3. X-ray crystal structure description

3.3.1. Crystal structure of H_2L salt with triethylamine

The single crystals of the ligand H_2L salt with triethylamine were obtained from the crystallization of the product obtained from an attempted synthesis of tin complex using this ligand in presence of triethyl amine base in methanol. Single crystals obtained from the recrystallization were analyzed and turned out to be the crystals of the azo-ligand salt with triethylamine base. The asymmetric unit of **H_2L** salt is outlined in Fig. 1 and the crystal data are presented in Table 1. There are two symmetrically independent molecules **A** and **B** in the asymmetric unit. Each 2-(4-hydroxynaphthylazo)-benzoic acid deprotonated at the carboxylic acid site with triethylammonium counter ions is solvated by water molecule. Despite the fact that the geometry (see Table 2) and conformation of both anions are similar, the search for higher symmetry with the PLATON program [31] did not give a positive result. The molecules are approximately planar with just small twists about the central C—N bonds linking the aromatic rings, as indicated by the torsion angles N(2)-N(1)-C(7)-C(6) = -2.9(4)° and N(1)-N(2)-C(8)-C(9) = 0.2(4)° for molecule **A** and N(4)-N(3)-C(27)-C(26) = -1.5(4)° and N(3)-N(4)-C(28)-C(29) = -1.6(4)° for molecule **B**, respectively. The deprotonated carboxylic acid groups are also coplanar with its parent phenyl ring [O(2)-C(1)-C(2)-C(3) = -173.1(3)° for **A** and O(5)-C(21)-C(22)-C(23) = -170.5(3)° for **B]**. In the solid state the hydrazone tautomeric form is observed for 2-(4-hydroxynaphthylazo)benzoic acid anion. This enables the formation of intramolecular hydrogen bonds of the N—H….O type (Table 3) between the oxygen atom from carboxylate group closest to the azo *N*-atom, which additionally stiffen the entire molecules (Fig. 1). The presence of water molecules and triethylamine cations in the structure leads to the formation of a series of N—H…O and O—H…O hydrogen bonds (Table 3, Fig. S1). As a result, a 2-D supramolecular structure of double-layer sheets of anions, with water and cations sandwiched in the middle, lie parallel to (0 1 0) is created. Finally, two intermolecular C—H…O interactions [C(4)-H(4)…O(5)$^{\#1}$; #1 = 1-x,1-y,2-z and C(24)-H(24)…O(2)$^{\#2}$; #2 = 1-x,1-y,1-z] serve to complete the supramolecular structure.

3.3.2. Crystal structure of Bu_3SnHL (1)

The complex **1** crystallizes in the trigonal system with non-centrosymmetric space group *R3c* [Flack parameter = -0.028(3)]. The molecular structure of complex **1** is shown in Fig. 2a. Selected bond lengths and bond angles are presented in Table 2. The compound **1** forms in solid state a highly zig-zag 1-D polymeric chain (Fig. 2b) in which the tin atom is five coordinated with the three butyl groups occupying the equatorial positions and the axial positions of trigonal bipyramid being occupied by a carboxylate oxygen, O(1) of azo-carboxylate ligand, and the phenolic oxygen, O(3)$^{\#3}$ [where #3 = 1/3-x + y,5/3-x,2/3 + z], of an adjacent molecule. The deformation of the

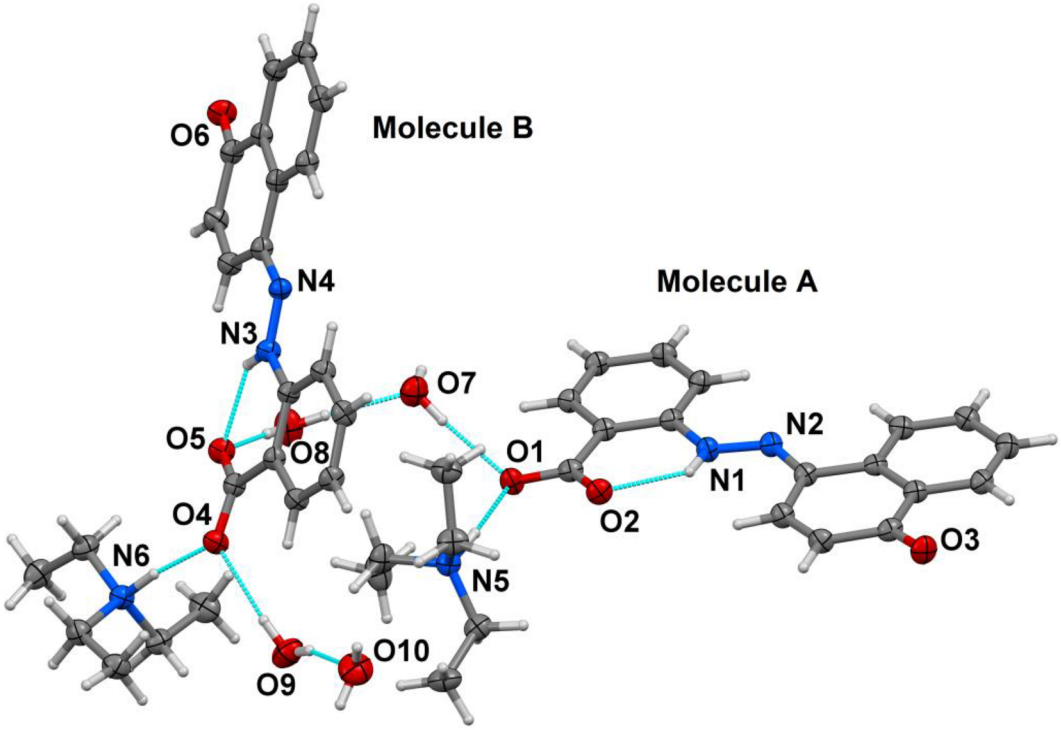

Fig. 1. The molecular structure and atom numbering scheme for **H_2L** salt with displacement ellipsoids drawn at 50% probability level.

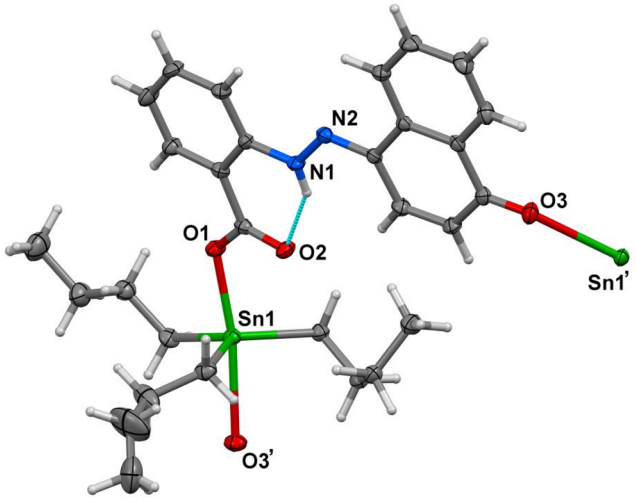

Fig. 2a. The molecular structure and atom numbering scheme for compound **1** with displacement ellipsoids drawn at 50% probability level.

Sn coordination sphere can be characterized quantitatively by parameter **τ** defined by Addison et al. [53]. The value of **τ** = (b-a)/60 [where b is the largest and a is the second largest basal angle around the Sn atom] for complex **1** is 0.79. This indicates a distorted trigonal bipyramidal geometry around Sn center. The sum of the C-Sn-C angles in the trigonal plane of the complex **1** is 355.89(11)°. The shorter Sn-$O_{carboxylate}$ distance Sn(1)-O(1) is 2.148(2)Å, while the Sn-$O_{phenolic}$ bond length Sn(1)-O(3)$^{\#1}$ is 2.537(3)Å. These values are within the range of Sn-O bond distances usually observed for organotin azo-carboxylate complexes [24,25,54]. The long Sn(1)….O(2) distance of 3.083(3)Å indicates that this oxygen atom is not involved in coordination with tin atom.

Apart from the occurring N—H…O intramolecular hydrogen bond (Table 3), there are no significant supramolecular interactions probably because of the azo-carboxylate ligands are not properly oriented for efficient π-π stacking (Fig. S2).

3.3.3. Crystal structure of $[(CH_3)_3Sn]_2(OH)(H_2O)HL$ (2)

The complex **2** crystallizes in the triclinic system with centrosymmetric space group *P*-1. As can be seen from Fig. 3, the asymmetric unit consists of complex $[(CH_3)_3Sn]_2(OH)(H_2O)HL$ and methanol molecules. Selected bond lengths and angles are listed in Table 2. In the crystal of **2**, no polymeric chain was formed, as found in the trimethyltin hydroxide [55]. To our knowledge, this kind of di-nuclear asymmetrical complex with single μ-O(H) bridge, has not been described in literature for organotin complexes yet. Each tin is pentacoordinate and the co-ordination environment is comprised of three methyl substituents, bridging hydroxy oxygen, carboxylate moiety for Sn(1) and oxygen atom of a water molecule for Sn(2), respectively. The coordination geometry around each tin is slightly distorted trigonal bipyramidal [the deformation parameters **τ** are 0.88 and 0.98 for Sn(1) and Sn(2) respectively], with the axial positions being occupied by one bridging hydroxy oxygen O(4) from μ-O(H) group and the carboxylate oxygen O (2) or water oxygen O(5) while the equatorial positions are taken up by the three carbons of the methyl substituents (Fig. 3). The two Sn atoms linked by the hydroxy group have similar co-ordination geometries, with short Sn-$O_{hydroxy}$ [2.188(5)Å and 2.136(5)Å] and longer Sn-$O_{carboxyl/water}$ [2.275(5)Å and 2.402(5)Å] bond distances, respectively. In each case the three methyl carbon atoms are slightly bent away from the shorter Sn-O(4) bond [mean bond angles C-Sn-$O_{hydroxy}$ = 93.2(2)° and C-Sn-$O_{carboxyl/water}$ = 86.7(2)°].

Just, like in the structure **1** the intramolecular hydrogen bond of the type N—H…O play an important role in stabilizing the structure of the complex. Besides, a 2-D H-bonding network in the direction (01–1) is created. The presence of methanol molecule, water molecule and hydroxy group coordinated to the Sn atoms enable the formation a number of intermolecular O—H…O hydrogen bonds (Table 3, Fig. S3).

3.3.4. Crystal structure of $[Bu_2Sn(HL)_2]_2$ (3)

The molecular structure of compound **3** is depicted in Fig. 4 while selected geometric parameters are given in Table 2. The complex **3** has two tin centers that are surrounded by two bidentate carboxylate groups and two butyl substituents. In addition, the Sn(1) atom forms a bond [Sn(1)-O(9) = 2.690(5)Å] with a hydroxy O atom of one azo-carboxylate ligand. Therefore, though uncommon, the coordination number is seven and six around Sn(1) and Sn(2), respectively. The donor atoms of the ligands are arranged in a distorted pentagonal bipyramidal conformation around Sn(1) with five oxygen atoms spanning the equatorial positions and two butyl carbon atoms at the apices of the bipyramid. The number of alkyl substituents involved in coordination to Sn(1) is probably the most important factor in fixing the geometry of the coordination polyhedron. Generally, when three alkyl groups are present in the organotin complex, they prefer an equatorial arrangement around Sn center in a trigonal bipyramid, while the presence of two alkyl groups, with the apparent necessity of maintaining two short

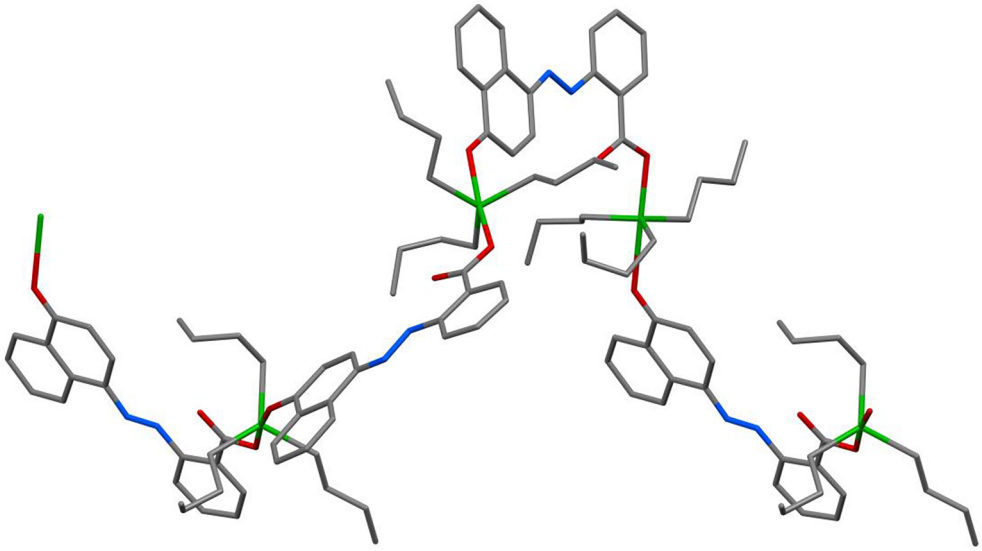

Fig. 2b. The 1-D infinite zig-zag polymeric chain of complex **1**.

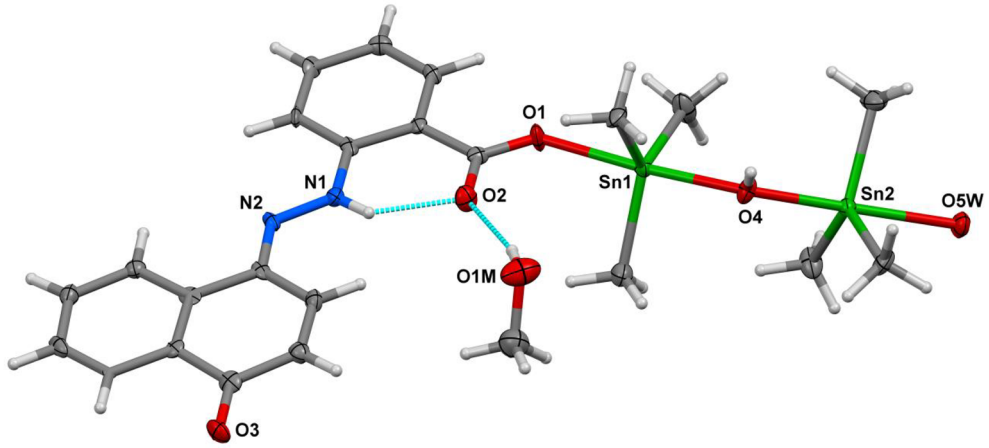

Fig. 3. The molecular structure and atom numbering scheme for compound **2**, with displacement ellipsoids drawn at the 50% probability level.

Sn-C bonds in apical positions, favors a pentagonal arrangement of the other ligands, allowing e.g. bidentate behavior of the carboxylate ions [56,57]. The five oxygen atoms O(1), O(2), O(4), O(5) and O(9) are coplanar with Sn(1) within the experimental errors. The Sn(2) atom adopts the skew-trapezoidal bipyramidal configuration. The carboxylate groups coordinate in an asymmetric mode around Sn(1) and Sn(2) centers forming four short Sn-O bonds [mean Sn-O = 2.135(4)Å] and four long Sn-O bonds [mean Sn-O = 2.520(5)Å]. The alkyl ligands lie in axial positions, thereby completing six-coordination around the Sn(2) atom. The bond angles of C-Sn-C [C(35)-Sn(1)-C(39) = 156.5(3)° and C(77)-Sn(2)-C(81) = 135.5(3)°] are close to the average found for diorganotin complexes in which the alkyl or aryl substituents do not adopt cis- or *trans*-geometries around the tin atom [58]. As in the case of compounds **1** and **2**, the structure **3** is stabilized by intramolecular hydrogen bonds of the N—H…O type (Table3, Figs. 4 and S4). No other significant supramolecular interactions were found.

3.4. Antidiabetic activity

Complexes **1** and **3** along with the ligand were screened for their antidiabetic activity against alpha glucosidase enzyme and the enzyme inhibition activities of these complexes were compared with standard compound acarbose. The results of the screening test of the anti-diabetic activity study against α-glucosidase enzyme revealed significant activity for the ligand $\mathbf{H_2L}$ and compound **1** in DMSO while compound **3** showed significant inhibition activity in ethanol. Therefore, inhibition concentration (IC_{50}) for the ligand $\mathbf{H_2L}$ in DMSO (LG_D) and compounds **1** (1_D) in DMSO and **3**(3_E) in ethanol were determined and compared with the standard drug, acarbose (Fig. 5). The results of the dose effect analysis (IC_{50}) of the ligand and compounds with acarbose are also summarized in Table 4. From the results of the dose analysis effect of the ligand and compounds, it was observed that compound **3** **(**C3_E**)** had higher enzyme inhibition activity (45.24 μg/mL) as

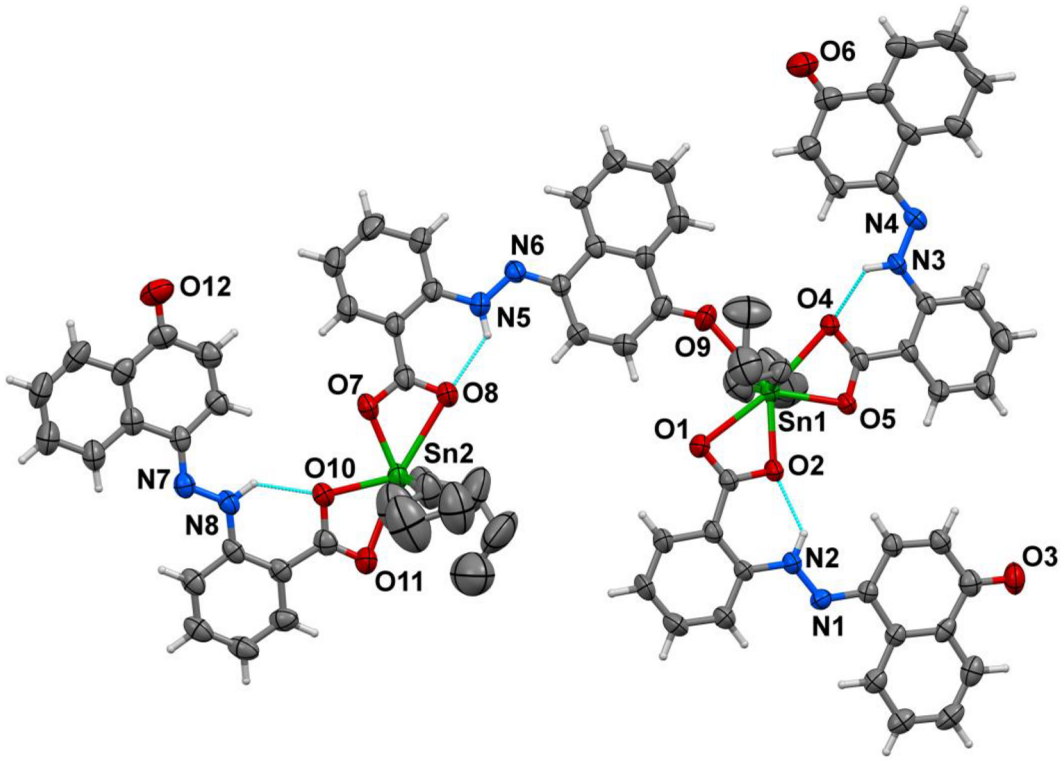

Fig. 4. The molecular structure and atom numbering scheme for compound **3**, with displacement ellipsoids drawn at the 30% probability level. Hydrogen atoms of the butyl groups have been omitted for clarity.

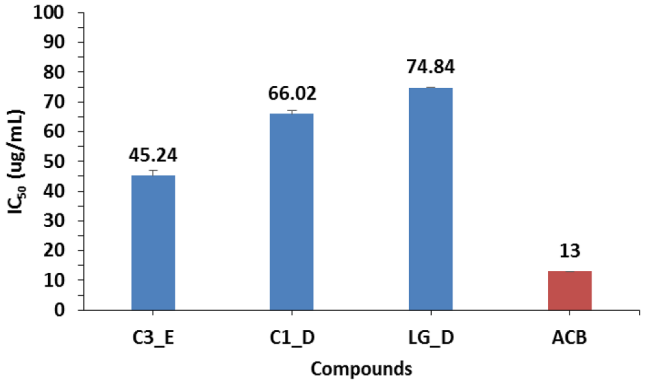

Fig. 5. IC_{50} values for ligand and compounds **1** or **3** along with standard compound acarbose against α-glucosidase.

Table 4
. Results of the enzyme inhibition activity (IC_{50}).

Compounds	IC_{50} (μg/mL)	SD (±)	Hill Co-efficient
1 (C1_D)	66.02	1.27	1.24 ± 0.54
3 (C3_E)	45.24	0.25	2.15 ± 0.35
H_2L (LG_D)	74.84	1.56	2.45 ± 0.53
Acarbose (ACB)	13.51	0.01	1.92 ± 0.78

compared to compound **1**(C1_D) which showed inhibition activity value at 66.24 μg/mL. Both the compounds displayed higher activity than ligand (LG_D) which showed IC_{50} value at 74.84 μg/mL. However, these compounds exhibited lower enzyme inhibition activity than standard compound acarbose (13 μg/mL). It is also clear from the results of the study that the Hill co-efficient value of the ligand and the compounds were found to be higher than 1.0 (Table 4) indicating positive co-operative binding of these compounds with the active sites of the enzyme and thus consequently leading to enzyme inhibition activity [25,59–61]. Thus, from this study it reveals that **3** (C3_E) has a significant α-glucosidase inhibition activity as compared to the ligand and compound **1**. However, the antidiabetic activity of the present series of the complexes were found to show lower activity than those related organotin(IV) compounds reported by our group earlier [22,23,25].

4. Conclusions

Synthesis of three triorganotin(IV) complexes **1–3** were accomplished by reacting 2-(4-hydroxynaphthylazo) benzoic acid with *bis*-tributyltin(IV) or dibutyltin(IV) oxide or trimethyltin(IV) chloride taking different molar reaction ratios . The complete characterization of the complexes was achieved by elemental analysis, IR and multinuclear NMR spectroscopy. Crystal structure analysis of the complexes revealed that compound **1** exhibits polymeric structure while **2** and **3** showed dinuclear structures. The geometry around tin atoms in **1** and **2** is best described as trigonal bipyramidal geometry while in **3** the geometry around tin atoms were found to be six-coordinate distorted skew trapezoidal and seven- coordinate pentagonal bipyramidal geometry respectively. NMR spectral study of the complexes suggested four coordinate structure for **1** and **2** while five coordinated structure is presumably adopted for **3** in solution thereby indicating dissociation of the solid state structures of these complexes into solution upon dissolution. The antidiabetic activities of the complexes were evaluated against alpha glucosidase enzyme and compared with standard compound. The result of the study reveals that compound **3** exhibited significant enzyme inhibition activity as compared to the ligand and compound **1**.

CRediT authorship contribution statement

Paresh Debnath: Methodology, Investigation, Writing - original draft. **Keisham Surjit Singh:** Supervision, Conceptualization, Writing - review & editing. **Thokchom Sonia Devi:** Investigation. **S.Sureshkumar Singh:** Formal analysis. **Ray J. Butcher:** Investigation. **Lesław Sieroń:** Investigation, Visualization. **Waldemar Maniukiewicz:** Writing - original draft, Writing - review & editing.

Declaration of Competing Interest

The authors declare that they have no known competing financial interests or personal relationships that could have appeared to influence the work reported in this paper.

Acknowledgements

Authors would like to thank SAIF, IIT Madras for providing crystal structure data for compound **3**, IISc, Bangalore for NMR spectra and DBT, Govt. of India (grant no. BT/32/NE/2011) for Biotech hub.

Appendix A. Supplementary data

Supplementary data to this article can be found online at https://doi.org/10.1016/j.ica.2020.119736.

References

[1] M. Gielen, Appl. Organomet. Chem. 16 (2002) 481.
[2] M. Gielen, E. R. T. Tiekink, in: M. Gielen, E. R. T. Tiekink (Eds.), Metallotherapeutic Drugs and Metal based Diagnostic Agents, Chapter 22: 50Sn Tin Compounds and their Therapeutic Potential, John Wiely& Sons Ltd., 2005, pp-421-439.
[3] M. Gielen, M. Biesemans, D. de Vos, R. Willem, J. Inorg. Biochem. 79 (2000) 139.
[4] D. Tzimopoulos, I. Sanidas, A.C. Varvogli, A. Czapik, M. Gdaniec, E. Nikolakaki, P.D. Akrivos, J. Inorg. Biochem. 104 (2010) 423.
[5] D.K. Dimertzi, V. Dokouro, A. Primikiri, R. Vergas, C. Silvestru, U. Russo, M.A. Dimertzis, J. Inorg. Biochem. 103 (2009) 738.
[6] V. Dokouro, A. Primikiri, D.K. Dimertzis, J. Inorg. Biochem. 105 (2011) 195.
[7] X.Y. Zhang, H.B. Song, Q.S. Lee, X.F. Liu, L.F. Tang, Polyhedron 26 (2007) 3743.
[8] G. Prabusankar, R. Murugavel, Organometallics 23 (2004) 5644.
[9] E.R.T. Tiekink, Appl. Organomet. Chem. 5 (1991) 1.
[10] E.R.T. Teikink, Trends Organomet. Chem. 1 (1994) 71.
[11] C. Ma, J. Sun, Dalton Trans. (2004) 1785.
[12] V. Chandrasekhar, C. Mohapatra, R.J. Butcher, Cryst. Growth Des. 12 (2012) 3285.
[13] C. Ma, Q. Jian, R. Zhang, D. Wang, Chem. Eur. J. 12 (2006) 420.
[14] R. García-Zarracino, H. Hopfl, J. Am. Chem. Soc. 127 (2005) 3120.
[15] T.S. Basu Baul, K.S. Singh, M. Holcapeck, R. Jirasko, E. Rivarola, A. Linden, J. Organomet. Chem. 690 (2005) 4232.
[16] T.S. Basu Baul, K.S. Singh, X. Song, A. Zapata, G. Eng, A. Lycka, A. Linden, J. Organomet. Chem. 689 (2004) 4702.
[17] T.S. Basu Baul, K.S. Singh, A. Lycka, A. Linden, X. Song, A. Zapata, G. Eng, Appl. Organomet. Chem. 20 (2006) 788.
[18] T.S. Basu Baul, W. Rynjah, E. Rivarola, A. Lycka, M. Holcapek, R. Jirasko, D. de Vos, R.J. Butcher, A. Linden, J. Organomet. Chem. 691 (2006) 4850.
[19] T.S. Basu Baul, A. Paul, L. Pellerito, M. Scopelliti, A. Duthie, D.de Vos, R.P. Verma, U. Englert, J. Inorg. Biochem. 107 (2012) 119.
[20] T.S. Basu Baul, A. Churasia, A. Duthie, P.M. Tolentino, H. Hopfl, Cryst. Growth Des. 19 (2019) 6656.
[21] M. Roy, S.S. Devi, S. Roy, C.B. Singh, K.S. Singh, Inorg. Chim. Acta 426 (2015) 89.
[22] M. Roy, S. Roy, K.S. Singh, J. Kalita, S.S. Singh, Inorg. Chim. Acta 439 (2016) 164.
[23] M. Roy, S. Roy, K.S. Singh, J. Kalita, S.S. Singh, New J. Chem. 40 (2016) 1471.
[24] P. Debnath, A. Das, K.S. Singh, T. Yama, S.S. Singh, R.J. Butcher, L. Sieroń, W. Maniukiewicz, Inorg. Chim. Acta 498 (2019) 119172.
[25] P. Debnath, K.S. Singh, K.K. Singh, S.S. Singh, L. Sieroń, W. Maniukiewicz, New J. Chem. 44 (2020) 5862.
[26] O.D. Rigaku, P.R.O. CrysAlis, Rigaku Oxford Diffraction Ltd, England, Oxford, 2019.
[27] Bruker. APEX2. Bruker AXS Inc., Madison, Wisconsin, USA, 2008.
[28] SMART and SAINT-PLUS. Area Detector Control and Integration Software. Versions 5.629 and 6.45, Bruker Analytical X-Ray Instruments Inc., Madison, WI, USA, 2003.
[29] G.M. Sheldrick, SHELXT - integrated space-group and crystal-structure determination, Acta Cryst. A71 (2015) 3.
[30] G.M. Sheldrick, Crystal structure refinement with SHELXL, Acta Cryst. C71 (2015) 3.
[31] A.L. Spek, PLATON SQUEEZE: a tool for the calculation of the disordered solvent contribution to the calculated structure factors, Acta Cryst. C71 (2015) 9.
[32] D. Kumar, H. Kumar, J.R. Vedasiromoni, B.C. Pal, Phytochem. Anal. 23 (2011) 421.

[33] D. Du, Z. Jiang, C. Liu, A.M. Sakho, D. Zhu, L. Xu, J. Organomet. Chem. 696 (2011) 2549.
[34] V. Dokorou, Z. Ciunik, U. Russo, D.K. Demertzi, J. Organomet. Chem. 630 (2001) 205.
[35] C. Ma, J. Li, R. Zhang, D. Wang, Inorg. Chim. Acta 359 (2006) 2407.
[36] C. Pettinari, F. Marchetti, R. Pettinari, D. Martini, A. Drozdov, S. Troyanov, Inorg. Chim. Acta 325 (2001) 103.
[37] T.P. Lockhart, F. Davison, Organometallics 6 (1987) 2471.
[38] A. Lyčka, J. Josef, N. Miroslav, Dyes pigments 15 (1991) 23.
[39] A. Lyčka, M. Valdimir, Dyes Pigments 7 (1986) 171.
[40] A. Lyčka, Dyes Pigments 43 (1999) 27.
[41] K.S. Singh, M. Roy, S. Roy, B. Ghosh, N.M. Devi, C.B. Singh, L.K. Mun, J. Coord. Chem. 70 (2017) 361.
[42] M. Nath, P.K. Saini, Dalton Trans. 40 (2011) 7077.
[43] M. Nadvornik, J. Holecek, K. Handler, A. Lycka, J. Ornganomet. Chem. 275 (1984) 43.
[44] J. Holecek, K. Handlir, M. Nadvornik, A. Lycka, J. Organomet. Chem. 258 (1983) 147.
[45] T.S. Basu Baul, A. Paul, A. Linden, J. Organomet. Chem. 696 (2012) 4229.
[46] M.M. Amini, A. Amirreza, R.K. Hamid, S.W. Ng, J. Organomet. Chem. 692 (2007) 3922.
[47] T.P. Lockhart, W.F. Manders, Inorg. Chem. 25 (1986) 893.
[48] J. Holecek, M. Nadvornik, K. Handlir, A. Lycka, J. Organomet. Chem. 315 (1986) 299.
[49] T.S. Basu Baul, W. Rynjah, E. Rivarola, C. Pettinari, A. Linden, J. Organomet. Chem. 690 (2005) 1413.
[50] J. Otera, T. Hinoishi, Y. Kawabe, R. Okawara, Chem. Lett. 10 (1981) 273.
[51] T.P. Lockhart, W.F. Manders, Inorg. Chem. 25 (1986) 892.
[52] T.P. Lockhart, Organometallics 7 (1988) 1438.
[53] A.W. Addison, T.N. Rao, J. Reedijk, J. Van Kijn, G.V. Verschoov, J. Chem. Soc., Dalton Trans. (1984) 1349.
[54] W. Maniukiewicz, E. Molins, C. Miravitlles, J.-C. Wallet, E.M. Gaydou, J. Chem. Cryst. 26 (1996) 691.
[55] K.M. Anderson, S.E. Tallentire, M.R. Probert, A.E. Goeta, B.G. Mendis, J.W. Steed, Cryst. Growth Des. 11 (2011) 820.
[56] H. Reuter, M. Reichelt, Can. J. Chem. 92 (2014) 471.
[57] M. Nardelli, C. Pelizzi, G. Pelizzi, J. Chem. Soc. Dalton Trans. (1978) 131.
[58] S.W. Ng, C. Wei, V.G. Kutnar Das, T.C.W. Mak, J. Organomet. Chem. 334 (1987) 295.
[59] H. d. A. Heck,, J. Am. Chem. Soc. 93 (1971) 23.
[60] D.L. Nelson, M.M. Cox, Lehninger Principles of Biochemistry, W. H. Freeman and Company, New York, pp. 162, 2008.
[61] H. Rehm, Protein Biochemistry and Proteomics, Academic Press, USA, 2006, pp. 59–69.